Feedback-assisted homodyne detection of phase shifts

Giacomo M. D'Ariano[*]

Department of Electrical and Computer Engineering, Northwestern University, Evanston, Illinois 60208

Matteo G. A. Paris[†]

Arbeitsgruppe ''Nichtklassiche Strahlung'' der Max-Planck-Gesellschaft an der Humboldt-Universität zu Berlin, Rudower Chaussee 5, 12489 Berlin, Germany

Raffaella Seno[‡]

Dipartimento di Fisica ''Alessandro Volta,'' Università degli Studi di Pavia, via A. Bassi 6, I-27100 Pavia, Italy

The problem of noise from external feedback control is addressed for homodyne detection of optical phase shifts. Two different schemes are analyzed: the conventional single-homodyne detection, and a two-quadrature scheme, which involves couples of independent measurements of two conjugated quadratures. The effectiveness of the feedback mechanism in both schemes is studied versus the feedback coupling parameter and high-sensitive detection regimes are discussed. The effect of nonunit quantum efficiency of photodetectors is also considered. It is shown that nonunit quantum efficiency affects phase sensitivity in the single-quadrature scheme to a larger extent than in the double-quadrature one. [S1050-2947(96)02411-0]

I. INTRODUCTION

The task of any phase detection scheme is to obtain the sharpest probability distribution with the minimum amount of photons impinging into the measuring apparatus. Historically this topic has stimulated a lot of theoretical work [1,2], however, with most effort devoted to the problem of a proper quantum mechanical definition of the phase, without paying much attention to the actual feasibility and simplicity of the detection scheme. In particular, homodyne detection still remains the most commonly adopted detector in any high-sensitive interferometry, but only a few approaches to this scheme viewed as a phase detector have been presented [3,4].

There are two main reasons why conventional homodyne detection have not attracted much attention from theoreticians. The first reason is that homodyning does not represent a kind of phase detection in a strict sense. In fact, the output photocurrent is proportional to a quadrature $\hat{x}_{\phi_0} = \frac{1}{2}(ae^{-i\phi_0} + a^{\dagger}e^{i\phi_0})$ of the field. Upon dividing $\hat{x}_{\phi_0}$ by the input field amplitude $|\langle a \rangle|$ (which should be known in advance) one has a knowledge of the phase shift ϕ only in the average sense, as $\langle \hat{x}_{\phi_0} \rangle = |\langle a \rangle|\cos(\phi - \phi_0)$, but a single outcome x of $\hat{x}_{\phi_0}$ still may correspond to an unreal phase when $x > |\langle a \rangle|$. Moreover, in this way only a single quadrature $\cos(\phi - \phi_0)$ is obtained, and hence ϕ turns out to be defined

in a π window, instead of a 2π one. The second reason is that the theoretical description of a homodyne detector is complicated by the need of a feedback to adjust the value of the reference phase (changing the phase of the local oscillator). The need of a feedback is conceptual—not just a technicality—because the sensitivity of the apparatus depends dramatically on the actual value of $\phi - \phi_0$, and the phase shift ϕ *a priori* is unknown. The feedback complicates the quantum description of the detector greatly, because now a single quantum outcome x in a series of repeated measurements depends on the past history of outcomes. Anyhow, neglecting the above difficulties (and considering the detector as working in the optimal-sensitivity region) it is well known that the phase sensitivity $\delta\phi \sim \langle \hat{n} \rangle^{-1}$ can be achieved for squeezed input states that have photons equally distributed between signal and squeezing: the possibility of such optimization, along with the relative simplicity of the scheme, are the main reasons why homodyne detection still remains so popular among experimentalists. However, as also shown in the following, the actual achievement of optimal sensitivity is still limited by nonunit quantum efficiency of detectors.

A way to overcome some theoretical difficulties arising in homodyne detection of the phase is to consider a scheme based on measurements of couples of conjugated quadratures, say $\hat{x}_{\phi_0}$ and $\hat{x}_{\phi_0 - \pi/2}$. In this case the knowledge of both quadratures $\cos(\phi - \phi_0)$ and $\sin(\phi - \phi_0)$ can be achieved without the need of knowing $|\langle a \rangle|$ *a priori*, and with ϕ correctly defined in a 2π window. In the following these schemes will be referred to as two-quadrature schemes, in contrast with the single-quadrature ones (based on conventional homodyne detection). Among the two-quadrature schemes we can distinguish the following two categories: (i) schemes based on *joint* measurements of the two quadratures (as double homodyne and heterodyne [5]); (ii) schemes based on *independent* measurements. Notice that conceptu-

---

*Permanent address: Dipartimento di Fisica ''Alessandro Volta,'' Università degli Studi di Pavia, via A. Bassi 6, I-27100 Pavia, Italy. Electronic address: dariano@pv.infn.it

†Permanent address: Dipartimento di Fisica ''Alessandro Volta,'' Università degli Studi di Pavia, via A. Bassi 6, I-27100 Pavia, Italy. Electronic address: paris@pv.infn.it

‡Electronic address: seno@pv. infn.it

ally any scheme for phase detection that is not based on *joint* quadrature measurements always needs more than one measurement of the phase shift, at least for setting the working point ϕ_0 for best sensitivity. The measurements are *independent* in the sense that they are performed on the same prepared input state, not on the state after state reduction from the preceding measurement (the latter is the case of the adaptive phase measurements recently introduced in Ref. [6]). This situation is common in experiments: in practice it means that the whole sequence of measurements is performed on a stable radiation source, well within the stability time of the source. Typically in current experiments (see, for example, quantum tomographic experiments [7]) up to 10^4-10^5 homodyne measurements at different reference phases ϕ_0 with respect to the local oscillator (LO) are performed within the stability time of the source. Hence, in practice, the only difference between one-quadrature and two-independent-quadrature schemes is that for the former ϕ_0 is always adjusted at the best sensitivity working point, whereas for the latter ϕ_0 is alternately shifted by $\pi/2$ every couple of measurements. Recent studies [8] have shown that *independent measurement schemes* can achieve ideal phase sensitivity $\delta\phi \sim \langle \hat{n} \rangle^{-1}$, but only for particular input states (weakly squeezed states with fixed orientation of the squeezing direction). On the other hand, *joint measurement schemes* have a sensitivity which is independent of the phase, but they suffer additional noise due to joint measurement [9], and can at most achieve phase sensitivity $\delta\phi \sim \langle \hat{n} \rangle^{-2/3}$ [10].

Hence, at the present status of art, there are two schemes which can achieve ideal sensitivity $\delta\phi \sim \langle \hat{n} \rangle^{-1}$: the conventional one-quadrature homodyne detection, and the unconventional two-quadrature homodyne detection with independent measurements. Both schemes need a feedback to keep detectors in the best sensitivity region. So, why use the two-quadrature scheme? There are two kinds of reasons. The more practical reason is that—for a number $\langle \hat{n} \rangle$ of input signal photons up to thousands—the two-quadrature scheme is less affected by nonunit quantum efficiency than the one-quadrature scheme: this will be shown in this paper on the basis of detailed numerical calculation. Secondly, the measurement of two quadratures allows a proper phase definition for each single experimental event [11].

Thus the aim of this paper is twofold. On one hand we give a detailed study of external feedback dynamics on the basis of Monte Carlo simulations of real experiments: in this way we will confirm the experimentalists' confidence that feedback-assisted homodyne detection provides a practically convenient way to measure phase shifts, but we give at the same time the actual performance of the feedback versus the feedback coupling and input photons $\langle \hat{n} \rangle$. On the other hand, we draw attention of experimentalists to a scheme based on couples of independent measurements of conjugated quadratures, showing that it provides a high-sensitive measurement of the phase for a wide range of values of quantum efficiency, input energy, and feedback parameter. Actually this scheme is no more difficult to realize than the single-quadrature one, because it just needs a phase shifter that switches between 0 and $\pi/2$ shifts.

The outline of the paper is the following. Section II is devoted to the conventional single-quadrature scheme, with
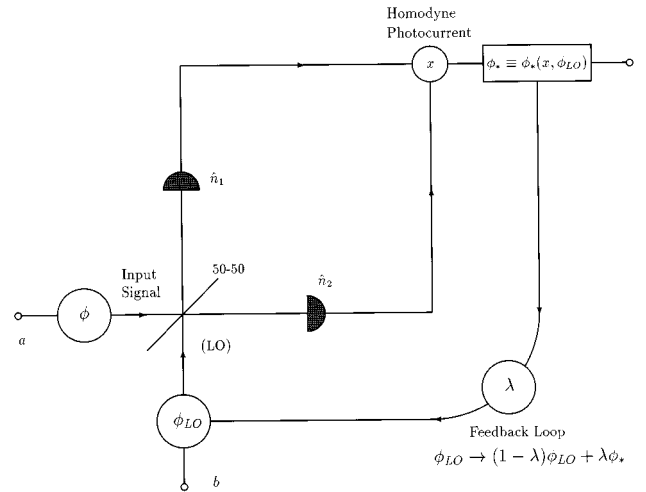

FIG. 1. Schematic outline of a feedback-assisted homodyne detector. The field mode a undergoes an unknown phase shift ϕ, to be measured. From each homodyne outcome x one extracts an estimation $\phi_* \equiv \phi_*(x; \phi_{LO})$ of ϕ. With the estimation ϕ_* the feedback loop adjusts the LO phase shift ϕ_{LO} according to the map $\phi_{LO} \to (1-\lambda)\phi_{LO} + \lambda\phi_*$.

results from Monte Carlo simulations in Sec. II A, and discussion on nonunit quantum efficiency in Sec. II B. Section III analyzes the two-quadrature scheme, and is structured in the same way as Sec. II. Section IV closes the paper with some concluding remarks.

II. SINGLE-QUADRATURE PHASE DETECTION

The homodyne detector is depicted in Fig. 1. The input mode a undergoes an unknown phase shift ϕ to be measured; a 50-50 beam splitter mixes the input with a LO at the same frequency of a prepared in a highly excited coherent state $|z\rangle$. The LO is time coherent with the input mode a, with a stable phase difference ϕ_{LO} relative to a. The output modes from the beam splitter are just the sum and difference of the input modes, and the difference photocurrent $\hat{I}_D = \hat{n}_2 - \hat{n}_1$ at zero frequency is detected, which in terms of the input modes is given by $\hat{I}_D = i(ab^\dagger - a^\dagger b)$ for an appropriate choice of the path lengths before detectors. In the strong LO limit $|z| \gg 1$ the reduced photocurrent $\hat{I}_D/|z|$ is just the quadrature $\hat{x}_{\phi_{LO}-\pi/2} \equiv \hat{I}_D/2|z|$, and thus the homodyne detector becomes a quadrature detector, with the LO playing the role of a stable classical reference for the phase.

We now consider squeezed states $|\alpha, \zeta\rangle$ at the input, with amplitude $\alpha = |\alpha|e^{i\phi}$ and squeezing parameter $\zeta = re^{i2\psi}$. As is shown in the following, the best sensitivity is achieved for ϕ_{LO} near to ϕ, whereas the sharpest probability distribution is obviously obtained when the direction ϕ of the detected quadrature $\hat{x}_\phi$ is the same as the direction of squeezing ψ: for this reason, in the following we will consider only states with $\psi = \phi$. For such states the probability distribution of the outcomes x of $\hat{x}_{\phi_{LO}-\pi/2}$ is the Gaussian

$$p(x;\phi_{LO};\phi)=\frac{1}{\sqrt{2\pi\Delta^2(\phi_{LO}-\phi)}}$$

$$\times\exp\left\{-\frac{[x-\bar{x}(\phi_{LO}-\phi)]^2}{2\Delta^2(\phi_{LO}-\phi)}\right\},\qquad(1)$$

with both average $\bar{x}$ and variance Δ^2 depending on $\varphi=\phi_{LO}-\phi$ as follows:

$$\bar{x}(\varphi)=|\alpha|\sin(\varphi),\qquad(2)$$

$$\Delta^2(\varphi)=\tfrac{1}{4}[\cosh(2r)-\sinh(2r)\cos(2\varphi)].\qquad(3)$$

From Eq. (3) it is clear that the sharpest distribution is reached when ϕ_{LO} coincides with the shift ϕ to be measured, whereas for fixed input photons $\langle\hat{n}\rangle$ the smallest variance $\Delta^2(0)$ is achieved for equal numbers of signal and squeezing photons, i.e., for $|\alpha|^2=\sinh^2 r=\langle\hat{n}\rangle/2$. On the contrary, for ϕ_{LO} different from ϕ the distribution (1) dramatically broadens: this situation is illustrated in Fig. 2, where we report $p(x;\phi_{LO};\phi)$ for $\phi=0$ at three different values of ϕ_{LO}.

Our aim is now to extract information on the phase ϕ from the random outcomes x in Eq. (1) or, more precisely, to define a measured *phase outcome* $\phi_*\equiv\phi_*(x;\phi_{LO})$ as a function of x at fixed ϕ_{LO}.

In particular, dealing with the homodyne detection scheme, from Eq. (2) one is tempted to adopt $\phi_*-\phi_{LO}=-\arcsin(x/|\alpha|)$, but there are still events with $|x|>|\alpha|$ for which no phase shift is defined. Usually these events are discarded, but they still carry the information that $\phi_*-\phi_{LO}\simeq\text{sgn}(x)\pi/2$. For this reason we adopt the definition

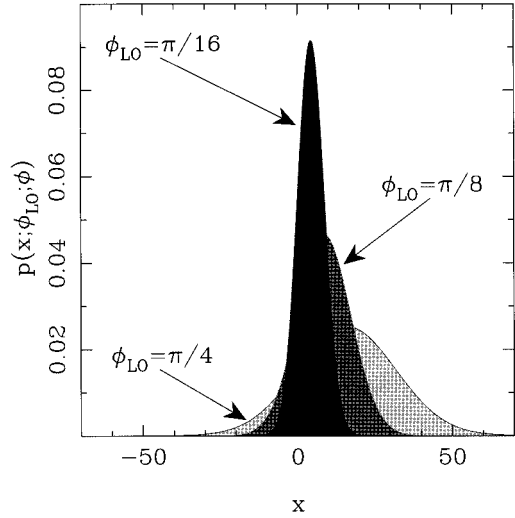
FIG. 2. Probability distribution $p(x;\phi_{LO};\phi)$ of the field quadrature $\hat{x}_{\phi_{LO}-\pi/2}$ for a squeezed state with an equal number of signal and squeezing photons ($|\alpha|^2=\sinh^2 r=500$), and with both signal and squeezing phases equal to zero. The probability distributions for three values of ϕ_{LO} are plotted.

$$\phi_*=\phi_{LO}-\arcsin\left(\frac{x}{|\alpha|}\right)\theta(|\alpha|-|x|)-\frac{\pi}{2}\text{sgn}(x)\theta(|x|-|\alpha|),$$
$$(4)$$

where $\theta(z)=1$ for $z\geq0$ and $\theta(z)=0$ for $z<0$. We emphasize that the choice of the phase for $|x|\geq|\alpha|$ actually is not relevant for highly excited input states, where such events become very rare. More relevant, on the contrary, is the fact that $\phi_*-\phi_{LO}$ is defined in a π window centered around zero, instead of a 2π window. The probability distribution of ϕ_* in Eq. (4) is given by

$$p(\phi_*;\phi_{LO};\phi)=\begin{cases}\dfrac{1}{2}-\dfrac{1}{2}\text{erf}\left[\dfrac{\sqrt{\langle\hat{n}\rangle}}{\Delta(\phi_{LO}-\phi)}[1\pm\sin(\phi_{LO}-\phi)]\right],&\phi_*=\phi_{LO}\pm\pi/2\\[4mm]\sqrt{\dfrac{\langle\hat{n}\rangle}{4\pi}}\dfrac{\cos(\phi_{LO}-\phi_*)}{\Delta(\phi_{LO}-\phi)}\exp\left\{-\dfrac{\langle\hat{n}\rangle[\sin(\phi_{LO}-\phi_*)-\sin(\phi_{LO}-\phi)]^2}{4\Delta^2(\phi_{LO}-\phi)}\right\}&\text{otherwise.}\end{cases}\qquad(5)$$

In Eq. (5) $\text{erf}(x)=(2/\sqrt{\pi})\int_0^x dt\,e^{-t^2}$ denotes the error probability function, and the distribution is normalized for $(\phi_{LO}-\phi_*)\in[-\pi/2,\pi/2]$.

A. Feedback-assisted measurements

As already observed, the closer ϕ_{LO} is to ϕ, the sharper the distribution (5). This can be qualitatively shown by the Gaussian approximation of (5) based on error propagation calculus. From Eq. (3) one obtains

$$|\phi-\phi_*|\approx\left|\frac{\delta(\phi-\phi_*)}{\delta\bar{x}}\right|_{\bar{x}=0}\delta\bar{x}$$

$$\approx\left|\frac{\delta(\phi-\phi_*)}{\delta\bar{x}}\right|_{\bar{x}=0}\Delta(\phi_{LO}-\phi)$$

$$\simeq\frac{1}{2\langle\hat{n}\rangle}[1+2\langle\hat{n}\rangle^2\sin^2(\phi_{LO}-\phi)].\qquad(6)$$

Unfortunately ϕ is the value that we want to measure, and

we do not know it in advance: thus a feedback loop to adjust the value of ϕ_{LO} is needed, otherwise the method becomes useless. Let ϕ_* denote the outcome of a measurement performed with a previously chosen value ϕ_{LO}: a linear feedback action which improves ϕ_{LO} for a subsequent measurement is described by the map

$$\phi_{LO} \to (1-\lambda)\phi_{LO} + \lambda\phi_*, \tag{7}$$

where $\lambda > 0$ is a coupling parameter. This is a kind of external feedback which acts on the path length of the local oscillator but does not affect the input mode. When applied for a sufficiently large number of measurement steps (of the same constant phase shift ϕ) the feedback mechanism (7) should drive ϕ_{LO} towards the optimum value $\phi_{LO} \equiv \phi$. Moreover, due to statistical deviations $\phi_* - \phi \neq 0$ around the "true" value ϕ, one expects that error propagation driven by the feedback from ϕ_* to ϕ_{LO} should produce a diffusion

process for both ϕ_* and ϕ_{LO}, thus adding noise to the stationary distribution (5) achieved with $\phi_{LO} = \phi$. As we will see in the following, such noise is vanishingly small for a large range of the parameter λ, and hence the feedback mechanism turns out to be very effective.

Let us describe in detail the evolution of the system driven by feedback (7). At the beginning there is no *a priori* knowledge of ϕ, and hence ϕ_{LO} is chosen at random with uniform probability distribution $p^{(0)}(\phi_{LO};\phi) = 1/2\pi$ (in the following, the parametric dependence of all probabilities on the true value ϕ is explicitly indicated). After the Nth measurement step the probability distribution $p^{(N)}(\phi_{LO};\phi)$ is improved by the feedback, starting from the previous one, $p^{(N-1)}(\phi_{LO};\phi)$. The iterative relation among probabilities can be obtained using Eq. (7) in terms of $p(\phi_*;\phi_{LO};\phi)$, which is just the probability density of ϕ_* *conditioned* by the LO phase shift ϕ_{LO}. One has

$$p_{LO}^{(N)}(\phi_{LO};\phi) = \int_{-\pi}^{\pi} d\phi_{LO}' \int_{\phi_{LO}' - \pi/2}^{\phi_{LO}' + \pi/2} d\phi_* p(\phi_*;\phi_{LO}';\phi) p_{LO}^{(N-1)}(\phi_{LO}';\phi) \delta_{2\pi}(\phi_{LO} - (1-\lambda)\phi_{LO}' - \lambda\phi_*), \tag{8}$$

where $\delta_{2\pi}$ denotes the 2π-periodic Dirac delta. Shifting the variable $\phi_* \to \phi_* - \phi_{LO}'$ leads to

$$p_{LO}^{(N)}(\phi_{LO};\phi) = \int_{-\pi}^{\pi} d\phi_{LO}' \int_{-\pi/2}^{\pi/2} d\phi_* p(\phi_* + \phi_{LO}';\phi_{LO}';\phi) p_{LO}^{(N-1)}(\phi_{LO}';\phi) \delta_{2\pi}(\phi_{LO} - \phi_{LO}' - \lambda\phi_*)$$

$$= \int_{-\pi/2}^{\pi/2} d\phi_* p(\phi_*(1-\lambda) + \phi_{LO};\phi_{LO} - \lambda\phi_*;\phi) p_{LO}^{(N-1)}(\phi_{LO} - \lambda\phi_*;\phi). \tag{9}$$

The *unconditioned* probability density of ϕ_* at the Nth measurement step is just the convolution of the conditional one with $p_{LO}^{(N-1)}(\phi_{LO};\phi)$, namely,

$$p^{(N)}(\phi_*;\phi) = \int_{-\pi}^{\pi} d\phi_{LO} p(\phi_*;\phi_{LO};\phi) p_{LO}^{(N)}(\phi_{LO};\phi). \tag{10}$$

Note that ϕ_*'s outcomes are distributed in a 2π window, even though $\phi_* - \phi_{LO}$ is confined in a π window.

The evolutions given by Eqs. (9) and (10) are illustrated in Fig. 3 on the basis of a Monte Carlo simulation for an input squeezed state with $\langle \hat{n} \rangle = 1000$. At the beginning ϕ_{LO} is randomly distributed, and thus the distribution of ϕ_* is very broad. For increasing N both $p^{(N)}(\phi_*;\phi)$ and $p_{LO}^{(N)}(\phi_{LO};\phi)$ exhibit a narrow central peak, with nonvanishing tails. Eventually, for large N the stationary distributions for both ϕ_* and ϕ_{LO} are Gaussian. The evolutions in the figure have been obtained for $\lambda = 0.2$. In the following we denote by N^* the number of measurement steps that are needed in order to reach the stationary distribution. Varying the value of λ two phenomena occur: on one hand for smaller λ one needs a larger N^* to reach stationary distributions; on the other hand the smaller λ, the sharper the final $p^{(N^*)}(\phi_*;\phi)$. The first assertion is illustrated in Fig. 4, where N^* is plotted versus λ for different values of $\langle \hat{n} \rangle$, and

where it is also apparent that N^* depends weakly on $\langle \hat{n} \rangle$. The second assertion is shown in Fig. 5, where the evolution of the rms width $\delta\phi_*^{(N)}$ of $p^{(N)}(\phi_*;\phi)$ is reported for two different values of λ. In the limit $\lambda \to 0$, numerical simulations show that phase sensitivity reaches the ideal bound

$$\delta\phi_* = \frac{1}{2\langle \hat{n} \rangle}, \tag{11}$$

however, the sensitivity (11) is achieved after an increasingly large number of steps. For finite values of λ the phase sensitivity is given by

$$\delta\phi_* = \frac{C(\lambda)}{\langle \hat{n} \rangle}, \tag{12}$$

where $C(\lambda)$ is an increasing function of λ: Eq. (12) shows that the feedback does not affect the power law for $\delta\phi_*$, but only changes the proportionality constant. In Fig. 6 the behavior of $C(\lambda)$ versus λ is reported, showing that for $\lambda < 1$ only very low noise is added, and thus the feedback loop is very effective.

On the basis of the previous numerical results we can now better understand the feedback mechanism using some analytical approximations valid for large $\langle \hat{n} \rangle \gg 1$. From Eqs. (4) and (5) we have
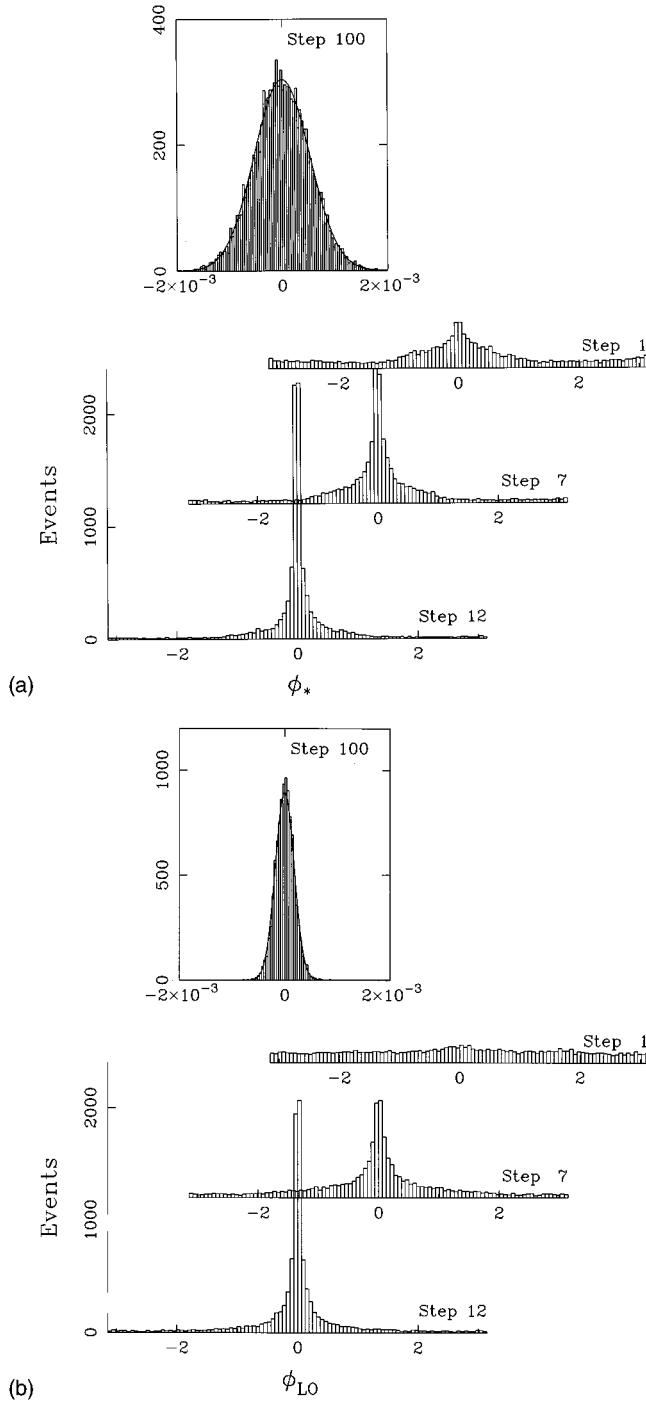
FIG. 3. Evolution of both the experimental distributions $p^{(N)}(\phi_*;\phi)$ and $p_{LO}^{(N)}(\phi_{LO};\phi)$ in Eqs. (9) and (10) from a Monte Carlo simulation of feedback-assisted homodyne measurements. The number of data collected in each step is 10^4. (a) Distributions $p^{(N)}(\phi_*;\phi)$ versus ϕ_* for $N=1,7,12$, and 100 (the last histogram is compared with a Gaussian). (b) Distributions $p_{LO}^{(N)}(\phi_{LO};\phi)$ versus ϕ_{LO} as in (a). The initial distribution $p^{(0)}(\phi_{LO};\phi)$ is set at random. All plots are obtained for $\lambda=0.2$, $|\alpha|^2=\sinh^2 r=500$, and $\phi=0$.

$$\phi_* \simeq \phi_{LO} - \frac{x}{|\alpha|}, \quad \phi_* - \phi \ll 1 . \tag{13}$$

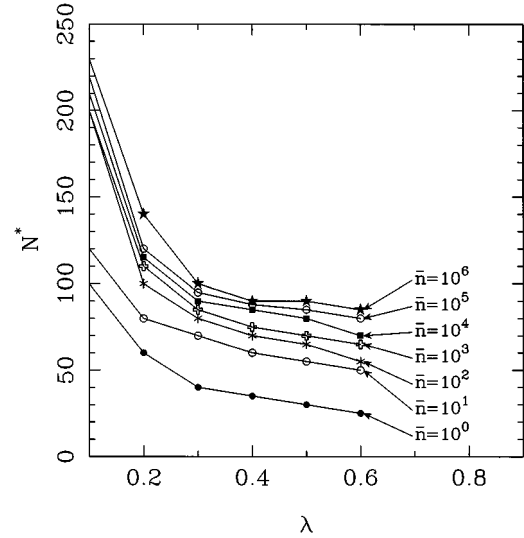The probability distribution (5) can be approximated by the Gaussian

FIG. 4. Number of steps N^* needed to reach the steady state, versus the feedback parameter λ for different input photon numbers $\bar{n}=\langle \hat{n} \rangle$.

$$p(\phi_*;\phi_{LO};\phi) \simeq \frac{1}{\sqrt{2\pi\sigma^2(\phi_{LO}-\phi)}} \exp\left[-\frac{(\phi_*-\phi)^2}{2\sigma^2(\phi_{LO}-\phi)}\right], \tag{14}$$

and variance $\sigma^2(\varphi)$ can be easily calculated for small feedback adjustments $\varphi=\phi_{LO}-\phi \ll 1$ using Eq. (3). One has

$$\frac{1}{\sigma^2(\varphi)} = \frac{\langle \hat{n} \rangle}{2\Delta^2(\varphi)} \simeq \frac{1}{\sigma^2(0)}\left(1 - \frac{\varphi^2}{\sigma^2(0)}\right), \tag{15}$$

where $\sigma(0)=1/(2\langle \hat{n} \rangle)$ is the ideal sensitivity (11). In addition, Monte Carlo simulation shows that the distribution $p_{LO}^{(N)}(\phi_{LO};\phi)$ itself is a Gaussian for $N \gtrsim N^*$, namely,
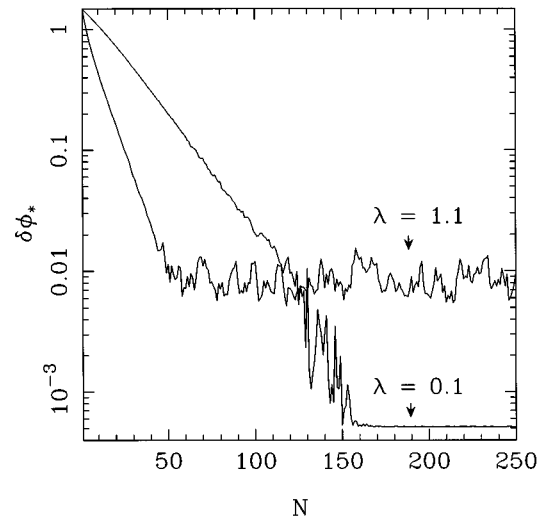

FIG. 5. Semilog plot of the rms width of $p^{(N)}(\phi_*;\phi)$ versus the number of feedback steps N for two different values of λ. The simulation is performed on a state with $\phi=0$, $|\alpha|^2=\sinh^2 r=500$, and with 10^5 data for each step.
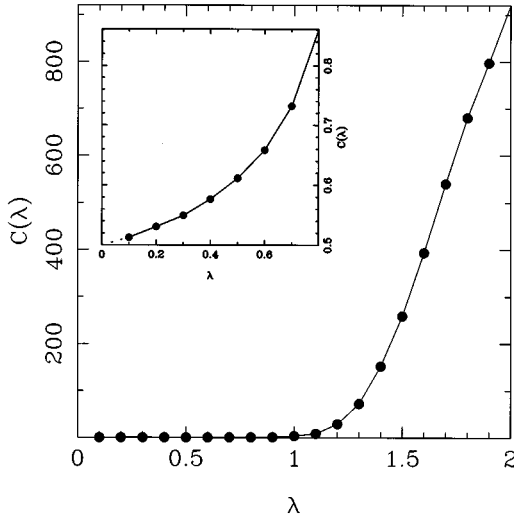
FIG. 6. Proportionality constant of the sensitivity power law $\delta\phi_* = C(\lambda)\langle\hat{n}\rangle^{-1}$ as a function of the feedback parameter λ. The inset is an amplification of the small λ's region, where feedback is more effective.

$$p_{LO}^{(N)}(\phi_{LO};\phi) \simeq \frac{1}{\sqrt{2\pi\delta\phi_{LO}^{(N)2}}}\exp\left[-\frac{(\phi_{LO}-\phi)^2}{2\delta\phi_{LO}^{(N)2}}\right]. \quad (16)$$

In the present approximation both $p^{(N)}(\phi_*;\phi)$ and $p_{LO}^{(N)}(\phi_{LO};\phi)$ can be considered as defined on the whole real axis instead of a 2π window. Using the evolution (9) and Eq. (14) for $p(\phi_*;\phi_{LO};\phi)$ it is easy to check that $p_{LO}^{(N)}(\phi_{LO};\phi)$ remains Gaussian for all subsequent steps. The width of this distribution evolves as follows:

$$\delta\phi_{LO}^{(N)} = |1-\lambda|\,\delta\phi_{LO}^{(N-1)} \sim e^{-N\lambda}\delta\phi_{LO}^{(0)}, \quad (17)$$

namely, asymptotically the feedback achieves an exponentially convergent sensitivity with rate proportional to λ^{-1} (the feedback parameter is confined in the interval $\lambda \in [0,2]$). The evolution of $p^{(N)}(\phi_*;\phi)$ can be calculated from Eqs. (10), (14), (15), and (16): a straightforward calculation shows that $p^{(N)}(\phi_*;\phi)$ is Gaussian to second order in $\langle\hat{n}\rangle^{-1}$, with variance

$$\delta\phi_*^{(N)} \simeq \sqrt{\sigma^2(0) + \delta\phi_{LO}^{(N)2}}$$

$$\simeq \sqrt{\sigma^2(0) + e^{-2N\lambda}\delta\phi_{LO}^{(0)}} \xrightarrow{N\gg N^*} \sigma(0). \quad (18)$$

Equation (18) is in agreement with Eq. (12), but the dependence of $C(\lambda)$ versus λ cannot be evaluated within the present analytical approximation.

B. Nonefficient detectors

When homodyne detector involves photocounters with nonunit quantum efficiency $\eta < 1$ the output probability distribution $p_\eta(x;\phi_{LO};\phi)$ becomes a Gaussian convolution of the ideal probability $p(x;\phi_{LO};\phi)$. One has
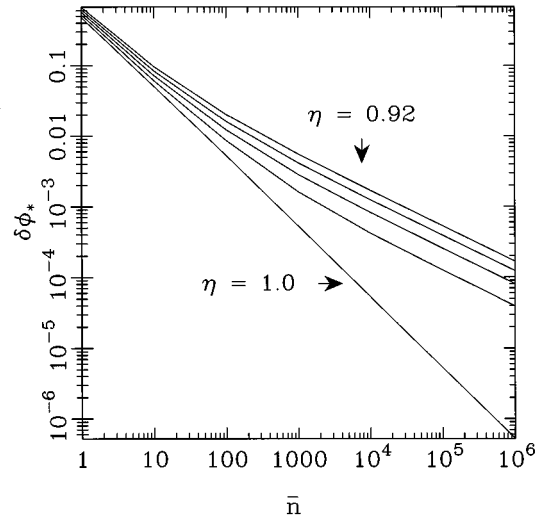

FIG. 7. Phase sensitivity $\delta\phi_*$ versus $\bar{n} = \langle\hat{n}\rangle$ from a Monte Carlo simulation of feedback-assisted homodyne measurements, for quantum efficiency $\eta = 1.0, 0.98, 0.96, 0.94$, and 0.92. The feedback coupling is $\lambda = 0.2$. The number N_* of steps used to reach the steady state is 100. The simulation is performed on a state with $\phi = 0$, $|\alpha|^2 = \sinh^2 r = 500$, and with 10^4 data for each step.

$$p_\eta(x;\phi_{LO};\phi) = \int_{-\infty}^{\infty} dx'\, p(x';\phi_{LO};\phi)\frac{1}{\sqrt{2\pi\Gamma_\eta^2}}$$

$$\times \exp\left[-\frac{(x'-x)^2}{2\Gamma_\eta^2}\right], \quad (19)$$

where the extra noise can be simply evaluated as [12,8]

$$\Gamma_\eta^2 = (1-\eta)/\eta. \quad (20)$$

Hence the output probability distribution still has the Gaussian shape (1), however, with the larger width

$$\Delta^2(\varphi) \rightarrow \Delta^2(\varphi) + \Gamma_\eta^2. \quad (21)$$

Nonunit quantum efficiency dramatically degrades phase sensitivity: the distribution $p_\eta(\phi_*;\phi_{LO};\phi)$ now is broader than $p(\phi_*;\phi_{LO};\phi)$ and for large $\langle\hat{n}\rangle$ Eq. (15) must be replaced with

$$\frac{1}{\sigma^2(\varphi)} = \frac{\langle\hat{n}\rangle}{2}[\Delta^2(\varphi) + \Gamma_\eta^2] = \frac{\langle\hat{n}\rangle}{2\Gamma_\eta^2}\left[1 - 4\frac{\langle\hat{n}\rangle}{\Gamma_\eta^2}\varphi^2\right]. \quad (22)$$

Upon substituting Eq. (22) in Eq. (19) [following the same lines for optimizing Eq. (18)] one is led to the shot noise sensitivity

$$\delta\phi_*^{(N)} \xrightarrow{N\gg N^*} \sqrt{\frac{2(1-\eta)}{\eta\langle\hat{n}\rangle}}. \quad (23)$$

Even though the feedback mechanism is still effective, it cannot overcome noise due to nonunit quantum efficiency. In Fig. 7 we report the phase sensitivity $\delta\phi$ versus $\langle\hat{n}\rangle$ for values of η slightly different from unit. The strong degradation of sensitivity is apparent: all curves for $\eta < 1$ converge to shot noise, and the asymptotic sensitivity (23) is actually

reached for a small number of photons $\langle \hat{n} \rangle$, roughly $\langle \hat{n} \rangle \gtrsim (1-\eta)^{-1}$, which is of order of tens also for high efficiency $\eta \gtrsim 0.9$.

III. TWO-QUADRATURE PHASE DETECTION

In this section we analyze a simple phase detection scheme based on independent measurements of couples of conjugated quadratures. As already shown in Refs. [8] for input squeezed states with squeezing aligned along the direction of the two quadratures, the joint probability distribution of the two quadratures is just the Wigner function, whereas its marginal phase probability can achieve ideal sensitivity $\delta \phi \sim \langle \hat{n} \rangle^{-1}$ for weak squeezing (only a few percentage of squeezing photons). This difference with respect to the one-quadrature scheme (where 50% of squeezing photons is needed) is due to the fact that the two-quadrature scheme is more sensitive to the tails of the phase probability distribution than the single-quadrature one. Here we study the two-quadrature scheme in the general case, namely, as a detector of an unknown phase shift ϕ, hence with the direction of squeezing ellipse arbitrary with respect to the two-quadrature frame. In this case the probability distribution of the two quadratures is no longer the Wigner function, and sensitivity is greatly degraded, similarly to the one-quadrature scheme. Again we need a feedback loop to drive the detector toward the optimum sensitivity region, and eventually the detector will measure the Wigner function only after a sufficiently

large number of steps. It is clear that, as for the one-quadrature case, the input state must be prepared with parallel directions for squeezing and signal, and so the same phase parameters of Sec. II will be adopted for the input state.

In the two-quadrature scheme each experimental event consists of a couple (x,y) of outcomes for the two conjugated quadratures $\hat{x}_{\phi_{LO}-\pi/2}$ and $\hat{x}_{\phi_{LO}}$. These two measurements are independently performed well within the stability time of the source (i.e., on the same prepared radiation input state). As the two measurements are independently performed, the joint probability distribution $w(x,y;\phi_{LO};\phi)$ is factorized as follows:

$$w(x,y;\phi_{LO};\phi)=p(x;\phi_{LO}-\pi/2;\phi)p(y;\phi_{LO};\phi), \quad (24)$$

with quadrature probabilities p given by Eqs. (1)–(3). The phase value inferred from each event is the polar angle of (x,y), namely,

$$\phi_* = \phi_{LO} - \arctan\left(\frac{y}{x}\right), \quad (25)$$

where arctan is evaluated between $-\pi$ and π, taking into account the individual signs of x and y. In this way ϕ_* is defined in a 2π window, and there is no need to know the amplitude $|\langle a \rangle| \equiv |\alpha|$ of the input field. The phase distribution is the marginal distribution of (24) integrated over the radius

$$m(\phi_*;\phi_{LO};\phi)=\int_0^\infty d\rho\,\rho\,w(\rho\,\cos(\phi_{LO}-\phi_*),\rho\,\sin(\phi_{LO}-\phi_*);\phi_{LO};\phi). \quad (26)$$

Substituting Eqs. (1)–(3) and (24) into Eq. (26) we obtain

$$m(\phi_*;\phi_{LO};\phi)=\frac{\exp[-\nu(\phi_{LO}-\phi)]}{4\pi\Delta(\phi_{LO}-\phi)\Delta(\phi_{LO}-\phi+\pi/2)\kappa(\phi_{LO}-\phi_*;\phi_{LO}-\phi)}$$
$$\times(1+e^{\tau^2(\phi_{LO}-\phi_*;\phi_{LO}-\phi)}\sqrt{\pi}\tau(\phi_{LO}-\phi_*;\phi_{LO}-\phi)$$
$$\times\{1+\text{erf}[\tau(\phi_{LO}-\phi_*;\phi_{LO}-\phi)]\}), \quad (27)$$

where

$$\kappa(\varphi_*;\varphi)=\frac{1}{2}\left[\frac{\cos^2\varphi_*}{\Delta^2(\varphi+\pi/2)}+\frac{\sin^2\varphi_*}{\Delta^2(\varphi)}\right], \quad (28)$$

$$\nu(\varphi)=\frac{|\alpha|^2}{2}\left[\frac{\cos^2\varphi}{\Delta^2(\varphi+\pi/2)}+\frac{\sin^2\varphi}{\Delta^2(\varphi)}\right], \quad (29)$$

$$\tau(\varphi_*;\varphi)=\frac{|\alpha|}{2}\left[\frac{\sin\varphi_*\cos\varphi}{\Delta^2(\varphi+\pi/2)}+\frac{\cos\varphi_*\sin\varphi}{\Delta^2(\varphi)}\right]\frac{1}{\sqrt{\kappa(\varphi_*;\varphi)}}. \quad (30)$$

The above distribution is very narrow and centered in $\phi_*=\phi$ for $\phi_{LO}=\phi$, whereas it shifts and rapidly broadens for ϕ_{LO} different from ϕ. In Fig. 8 we report the distribution $m(\phi_*;\phi_{LO};\phi)$ of a squeezed state with $\phi=0$ and for different values of ϕ_{LO} and $\sinh^2 r=0.05\langle \hat{n} \rangle$ (only a few percent of squeezing is needed, see Refs. [8]).

For $\phi_{LO}=\phi$ (i.e., when we measure exactly the two quadratures corresponding to principal squeezing axes) the factorized distribution (24) coincides with the Wigner function $W_0(\alpha,\bar{\alpha})$ of the input field, namely,

$$w(x,y;\phi;\phi)\equiv W_0(x+iy,x-iy)$$
$$=\frac{1}{2\pi\sigma_1\sigma_2}\exp\left[-\frac{(x-|\alpha|)^2}{2\sigma_1^2}-\frac{y^2}{2\sigma_2^2}\right], \quad (31)$$
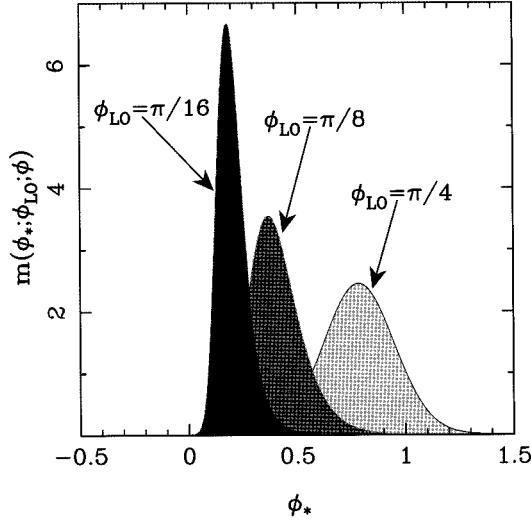
FIG. 8. Marginal phase distribution $m(\phi_* ; \phi_{LO} ; \phi)$ for two-quadrature homodyne detection with input squeezed state with $\langle \hat{n} \rangle = 1000$ and squeezing photons $\sinh^2 r = 0.05$. Both signal and squeezing phases are set to zero. The distributions for three different values of ϕ_{LO} are reported.

where

$$\sigma_1^2 = \frac{1}{4} e^{2r}, \quad \sigma_2^2 = \frac{1}{4} e^{-2r}. \tag{32}$$

However, ϕ is just the quantity that we want to measure, and we need a feedback loop as in Eq. (7) in order to adjust ϕ_{LO}.

The uncertainties in Eq. (32) are the true intrinsic quantum uncertainties of the squeezed state: no additional noise has been added by the measurement, as for the 3 dB added noise of joint measurement. The absence of added noise results from independence of the two homodyne measurements. One should stress, however, that the price to pay here is the need of twice the number of measurements with respect to the joint measurements case (see also note [10]).

A. Feedback-assisted measurements

The feedback mechanism (7) acts in the two-quadrature scheme in a way similar to the single-quadrature one. One has the unconditioned probability distribution in the complex plane

$$w^{(N)}(x,y;\phi) = \int_{-\pi}^{\pi} d\phi_{LO} w(x,y;\phi_{LO};\phi) p_{LO}^{(N)}(\phi_{LO};\phi), \tag{33}$$

and the unconditioned marginal phase probability after N steps is given by a convolution analogous to (10),

$$m^{(N)}(\phi_* ;\phi) = \int_{-\pi}^{\pi} d\phi_{LO} m(\phi_* ;\phi_{LO};\phi) p_{LO}^{(N)}(\phi_{LO};\phi), \tag{34}$$
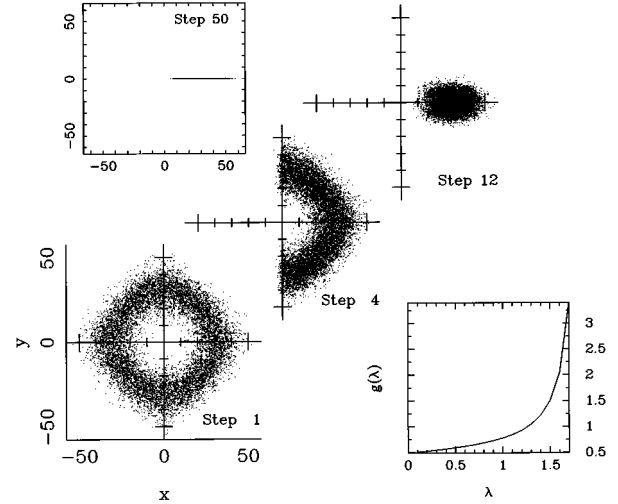

FIG. 9. Evolution of the experimental distribution $w^{(N)}(x,y;\phi)$ in the complex plane from a Monte Carlo simulation of two-quadrature feedback-assisted measurement with $\lambda = 0.2$. The number of data collected in each step is 10^4. The distributions for $N = 1, 4, 12,$ and 50 are reported. In all plots $\phi = 0$, $\langle \hat{n} \rangle = 1000$, and the number of squeezing photons is set equal to $0.05 \langle \hat{n} \rangle$; the local oscillator phase is initially distributed at random. The lower inset shows the behavior of the function $g(\lambda)$ which appears in the stationary variance $\Delta y = g(\lambda) e^{-r}$ of the $w^{(N)}(x,y;\phi)$ distribution.

with $m(\phi_* ;\phi_{LO};\phi)$ given by Eq. (26). Similarly, the LO phase shift probability after N feedback adjustments is given by

$$p_{LO}^{(N)}(\phi_{LO};\phi) = \int_{-\pi}^{\pi} \frac{d\phi_*}{1-\lambda} m\left(\phi_* ; \frac{\phi_{LO} - \lambda \phi_*}{1-\lambda}; \phi \right)$$

$$p_{LO}^{(N-1)}\left(\frac{\phi_{LO} - \lambda \phi_*}{1-\lambda}; \phi \right). \tag{35}$$

In Fig. 9, we report the results of a Monte Carlo simulation of the feedback-assisted evolution of the unconditioned distribution $w^{(N)}(x,y;\phi)$ for $\phi = 0$ and for initial distribution $p_{LO}^{(0)}(\phi_{LO};\phi)$ set at random. At the beginning the distribution $w^{(1)}(x,y;\phi)$ is very delocalized in the complex plane, with a ring shape around the origin, corresponding to no information on the phase. During the evolution, the distribution shrinks approaching the limiting distribution $W_0(x+iy,x-iy)$ after a sufficiently high number N of steps. In order to check convergence of the distribution in the complex plane, we evaluate the variance Δy at each step, and we find that after a sufficiently large number of steps Δy converges to a stationary value $\Delta y = g(\lambda) e^{-r}$. For the Wigner function one has $\Delta y = 1/2 e^{-r}$, whereas in practice $g(\lambda)$ is larger than 1/2, reflecting the noise added by the feedback. The behavior of $g(\lambda)$ is also reported in Fig. 9. It is close to 1/2 for a wide range of values of λ, showing that feedback adds a very low noise. For $\lambda \to 0$ the noise vanishes: however, the smaller is λ, the greater is the number N^* of steps needed to reach the steady state.

In Fig. 10, the corresponding marginal phase distribution $m^{(N)}(\phi_* ;\phi)$ is reported. This starts with a central peak in the middle of high and broad tails, it narrows during the
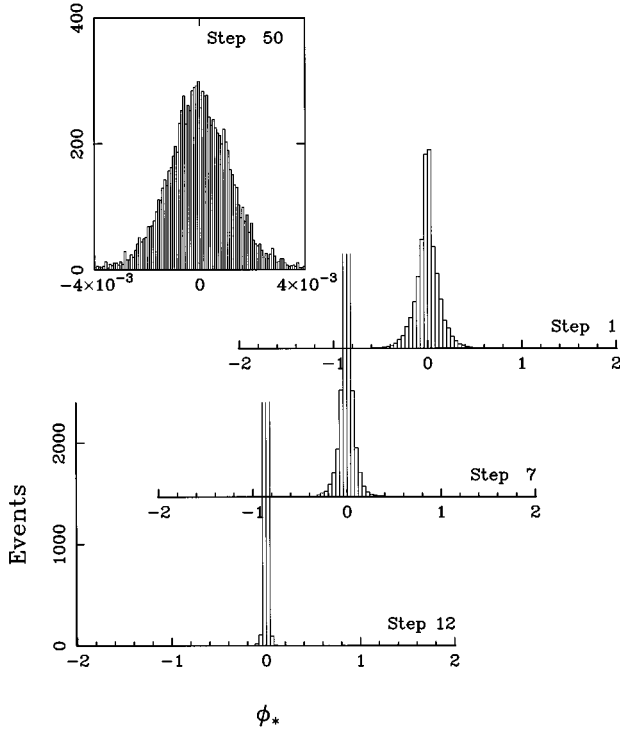
FIG. 10. Evolution of the marginal phase distribution $m^{(N)}(\phi_*;\phi)$ from the same Monte Carlo simulation as in Fig. 9.

transient, and eventually approaches the steady distribution in Eq. (27) for $\phi=\phi_{LO}$ after a sufficiently large number of steps. The phase sensitivity is given by $\delta\phi_* \sim \langle\hat{n}\rangle^{-1}$, with a proportionality constant which approaches unit for decreasing λ (see also Fig. 11).

B. Nonefficient detectors

Nonunit quantum efficiency η of the photodetectors causes the probability distribution of each measured quadrature to become a Gaussian convolution of the corresponding distribution for $\eta=1$. The probability distribution in the complex plane is given by

$$w_\eta(x,y;\phi_{LO};\phi)=p_\eta(x;\phi_{LO}-\pi/2;\phi)p_\eta(y;\phi_{LO};\phi),$$
(36)

where $p_\eta(x;\phi_{LO};\phi)$ is given in Eq. (19). The feedback mechanism is still effective in the presence of nonefficient detectors, and the unconditioned distribution

$$w_\eta^{(N)}(x,y;\phi)=\int_{-\pi}^{\pi}d\phi_{LO}w_\eta(x,y;\phi_{LO};\phi)p_{LO}^{(N)}(\phi_{LO};\phi)$$
(37)

reaches a stationary distribution after a number N^* of steps (which is almost the same as for $\eta=1$). The limiting distribution is now given by a generalized Wigner function [13]
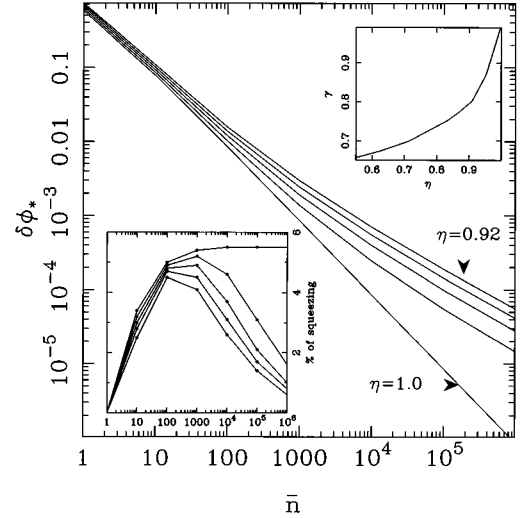
$$w_\eta(x,y;\phi;\phi)\equiv W_s(x+iy,x-iy)$$

FIG. 11. Phase sensitivity $\delta\phi_*$ versus $\langle\hat{n}\rangle$ from a Monte Carlo simulation of feedback-assisted double-homodyne measurements, for the same values of η as in Fig. 7. The feedback coupling is $\lambda=0.2$, and the number N_* of steps used to reach the steady state is 50. The simulation is performed on a state with $\phi=0$, $\langle\hat{n}\rangle=1000$, $\sinh^2 r=50$, and for 10^4 data at each step. The lower inset reports the optimal squeezing fraction relative to each value of the quantum efficiency η. The upper curve is for $\eta=1$. The upper inset reports the exponent γ of the phase sensitivity power law $\delta\phi\sim\langle\hat{n}\rangle^{-\gamma}$ as a function of the quantum efficiency η for $\langle\hat{n}\rangle$ running from 100 to 1000.

$$=\frac{1}{2\pi\sigma_1\sigma_2}\exp\left[-\frac{(x-|\alpha|)^2}{2\sigma_1^2}-\frac{y^2}{2\sigma_2^2}\right],$$
(38)

with

$$\sigma_1^2=\frac{1}{4}(e^{2r}-s),\quad \sigma_2^2=\frac{1}{4}(e^{-2r}-s),$$
(39)

where the ordering parameter s is given by $s=1-\eta^{-1}$: this distribution is broader than $W_0(x+iy,x-iy)$, and is given by the Gaussian convolution of W_0,

$$W_{1-\eta^{-1}}(\alpha,\bar{\alpha})=\int_C\frac{d^2\beta}{\pi[(1-\eta)/\eta]}W_0(\beta,\bar{\beta})$$
$$\times\exp\left\{-\frac{|\alpha-\beta|^2}{(1-\eta)/\eta}\right\}.$$
(40)

The phase distribution $m_\eta^{(N)}(\phi_*;\phi)$ approaches the marginal phase distribution of Eq. (38) for a sufficiently large number of steps. For squeezed optimized states with number of photons limited by the relation

$$\langle n\rangle\lesssim\frac{1}{\alpha_{opt}(1-\eta)},$$

where $\alpha_{opt}=\sinh^2 r/\langle n\rangle$ is the optimum fraction of squeezing photons ($\alpha\sim0.05$, it means $\langle n\rangle$ up to thousands for efficient detectors $\eta\gtrsim0.9$) the phase distribution exhibits a sensitivity

which scales as $\delta\phi\sim\langle\hat{n}\rangle^{-\gamma}$, where the exponent γ is a function of the quantum efficiency. On the other hand, for larger $\langle\hat{n}\rangle$ it can be shown from Eq. (27) that the asymptotic sensitivity is again shot noise limited. However, differently from the single-quadrature scheme, there is now a large range of $\langle\hat{n}\rangle$ where one has only a smooth degradation of the ideal sensitivity. It is also worth remembering that here only a few percentage of squeezing photons is needed, whereas for the one-quadrature scheme it is 50%. In Fig. 11 we report the phase sensitivity originated from feedback-assisted measurements with different values of the quantum efficiency η. We also report the optimal squeezing photon fraction, along with the behavior of the exponent γ as a function of η in the low $\langle\hat{n}\rangle$ region.

IV. CONCLUSION

In this paper we have studied two feedback-assisted detection schemes for the phase shift of a squeezed state of radiation. Both schemes are based on homodyne detection, but in one case a single field quadrature $\hat{x}_\phi$ is detected, whereas in the other each experimental event is a couple of independent measurements of two conjugated quadratures $\hat{x}_\phi$ and $\hat{x}_{\phi-\pi/2}$. The dynamics for both schemes have been extensively studied numerically, showing that the external feedback mechanism is very effective, and introduces a negligible noise for a wide range of the coupling parameter. Smaller values of the coupling parameter produce a lower additional noise, however, they need a larger number of steps to reach the steady state. The case of nonunit efficiency at photodetectors has also been considered, showing that the feedback mechanism still works, and is not affected by the detection noise. The performance of the two schemes in this realistic situation has been analyzed in detail.

In the single-quadrature scheme the resulting phase sensitivity is given by the power law $\delta\phi_* = C(\lambda)/\langle\hat{n}\rangle$ versus the input energy $\langle\hat{n}\rangle$, where $C(\lambda)$ is less than unit for $\lambda<1$, and achieves the minimum value $C(\lambda)=\frac{1}{2}$ for $\lambda\to0$. Hence the feedback-assisted measurement exhibits the ideal sensitivity, apart from a proportionality constant. When nonefficient detectors are involved, the feedback control is still effective, however, it cannot clean out the extra noise due to quantum efficiency: in this case the phase sensitivity dramatically degrades, and becomes shot noise limited for $\langle\hat{n}\rangle\gtrsim(1-\eta)^{-1}$. This difficulty can be partially overcome by means of the second scheme, which is based on couples of homodyne measurements. Here the feedback drives the joint probability distribution of two quadratures towards the Wigner function $W_0(\alpha,\overline{\alpha})$ of the input state, and it is effective for a wide range of the coupling parameter. The corresponding marginal phase distribution exhibits an ideal sensitivity apart from a proportionality constant, which is affected by the feedback noise. When nonefficient detectors are involved, the probability distribution of the two quadratures becomes broadened, and approaches the Wigner function $W_{1-\eta^{-1}}(\alpha,\overline{\alpha})$ after a sufficiently large number of steps. The marginal phase distribution has a sensitivity $\delta\phi\sim\langle\hat{n}\rangle^{-\gamma}$. For not too large number of photons the exponent γ is not far from unit for a broad range of the quantum efficiency η. The states which achieve this optimal sensitivity require only a few percent of photons engaged in squeezing, and this fraction decreases for decreasing η. Therefore we conclude that the two-quadrature scheme can be used in practice to improve the phase sensitivity, and we propose it for experimental investigations.

[1] Phys. Scr. **T48** (1993) special issue on quantum phase and phase dependent measurements, edited by W. Schleich and S. M. Barnett, and references therein.
[2] R. Lynch, Phys. Rep. **256**, 367 (1995).
[3] W. Vogel and W. Schleich, Phys. Rev. A **44**, 7642 (1991).
[4] J. W. Noh, A. Fougeres, and L. Mandel, Phys. Rev. A **45**, 424 (1992).
[5] G. M. D'Ariano and M. G. A. Paris, Phys. Rev. A **49**, 3022 (1994).
[6] H. M. Wiseman, Phys. Rev. Lett. **75**, 4587 (1995).
[7] D. T. Smithey, M. Beck, M. G. Raymer, and A. Faridani, Phys. Rev. Lett. **70**, 1244 (1993).
[8] G. M. D'Ariano, C. Macchiavello, and M. G. A. Paris, Phys. Lett. A **195**, 286 (1995).
[9] H. P. Yuen, Phys. Lett. **91A**, 101 (1982).
[10] Actually they need half as many measurements as schemes based on independent measurements, but the factor of 2 does not repay the optimal power law $\delta\phi\sim\langle\hat{n}\rangle^{-1}$ for sufficiently large $\langle\hat{n}\rangle$.
[11] In this paper we do not deal with the problem of defining a quantum phase observable (see Ref. [1]), but we adopt an operational point of view [4] that consists in defining the phase outcome from the prescription for the measuring procedure. It is worth noticing that it is now widely accepted that a unique operational definition of a quantum phase observable cannot be given. The best approach to the problem is that of quantum estimation theory (see also Ref. [5]), based on probability operator-valued measures (POM) generalizing orthogonal resolutions of the identity from customary self-adjoint observables. In the present case we are in a situation more similar to the one of optical homodyne tomography [7], where a set of inequivalent operators are independently measured. In such a case a POM description would consist of an overcomplete resolution of the identity based on many different orthogonal resolutions parametrized by an additional parameter (the phase ϕ_0 that labels different quadratures of the field).
[12] U. Leonhardt and H. Paul, Phys. Rev. A **48**, 4598 (1993).
[13] The generalized Wigner distribution function $W_s(\alpha,\overline{\alpha})$ in the phase space is defined as

$$W_s(\alpha,\overline{\alpha})=\int (d^2\lambda/\pi^2)e^{\alpha\overline{\lambda}-\overline{\alpha}\lambda+(1/2)s|\lambda|^2}\,\mathrm{Tr}(\rho e^{\lambda a^\dagger-\overline{\lambda}a})\ .$$